Molecular Crystals and Liquid Crystals Science and Technology. Section A. Molecular Crystals and Liquid Crystals

Publication details, including instructions for authors and subscription information:
http://www.tandfonline.com/loi/gmcl19

Optimization of Film Compensated Reflective Bistable Twisted Nematic Liquid Crystal Displays

Hongfei Cheng [a] & Hongjin Gao [a]

[a] Center of Liquid Crystal Technology, Department of Chemistry, Tsinghua University, Beijing, 100084, People's Republic of China

Version of record first published: 24 Sep 2006

To cite this article: Hongfei Cheng & Hongjin Gao (2001): Optimization of Film Compensated Reflective Bistable Twisted Nematic Liquid Crystal Displays, Molecular Crystals and Liquid Crystals Science and Technology. Section A. Molecular Crystals and Liquid Crystals, 369:1, 83-94

To link to this article: http://dx.doi.org/10.1080/10587250108030011

Mol. Cryst. Liq. Cryst., Vol. 369, pp. 83-94
Reprints available directly from the publisher
Photocopying permitted by license only

Optimization of Film Compensated Reflective Bistable Twisted Nematic Liquid Crystal Displays

HONGFEI CHENG* and HONGJIN GAO

Center of Liquid Crystal Technology, Department of Chemistry, Tsinghua University, Beijing 100084, People's Republic of China

(Received June 06, 2000; In final form February 21, 2001)

The operation modes of reflective bistable twisted nematic (BTN) liquid crystal displays were analyzed for both front and rear film compensations. The film compensated BTN displays shows rich operation modes. Several typical operation conditions were studied for their wavelength dispersions. The optimum conditions of the film compensated reflective BTN displays could have large values of $d\Delta n$ compared to those of non-compensated reflective BTN displays.

Keywords: bistable twisted nematic; reflective display; liquid crystal display; film compensation; optimization

1. INTRODUCTION

Bistable twisted nematic (BTN) displays were first discovered by Berremen and Heffner.[1,2] The BTN displays switched between two metastable twisted nematic states. The two bistable twist angles were 0 and 2π. If the applied voltage is switched off slowly, the liquid crystal relaxes to the 0 twisted state. When the applied voltage is switched off suddenly, the liquid crystal relaxes to the 2π twisted state due to the "back flow" effect.[2]

In 1995, a high quality passive matrix driven BTN display with a large number of scanning lines was realized by Tanaka et al.[3] Since then, the BTN display has attracted great attention and several detailed studies on the bistable mechanism have been reported.[4–8] These BTN displays have very large viewing angle since both metastable twist states of the BTN display have in-plane alignment.

* Author to whom correspondance should be addressed.

Because of the bistable effect, a BTN display can be multiplex driven with good image quality and minimum cross-talk.

A single polarizer reflective bistable twisted nematic liquid crystal display was reported recently.[9] Reflective liquid crystal displays are attractive for many display applications, particularly when an opaque back substrate such as silicon is used for electrically addressing a pixel. In many reflective displays two polarizers are used. In this case absorption losses reduce the efficiency of the devices. The single polarizer configuration is therefore preferred in reflective displays.

In our previous article, the optical properties were studied for the reflective BTN displays.[10] The results of numerical study of film compensated reflective BTN liquid crystal displays will be presented in this paper. This paper emphasizes the optical properties of such displays. Both front and rear film compensated reflective BTN displays will be studied in this paper.

2. PARAMETER SPACE OF REFLECTIVE BTN DISPLAYS

The parameter space method was used to characterize the operational modes of a reflective BTN liquid crystal display.

In order to motivate the parameter studies we will describe the physics of a BTN device. If the surface boundary conditions of a liquid crystal display favor a twist of ϕ in the liquid crystal material and the natural twist of the LC, as controlled by a chiral dopant, is $\phi+\pi$, then twists of ϕ and $\phi+2\pi$ will have the same deformation energy. To switch a $\phi+\pi$ twisted cell, the reset state must be generated before applying a selection pulse. When a reset pulse is applied, the initial $\phi+\pi$ twisted state changes to the vertically-aligned homeotropic state, because the liquid crystal tends to align parallel to the applied electric field. In the reset state, a selection pulse following the reset pulse can select a stable state that persists for hundreds of milliseconds.[9] The final state depends on the magnitude of the selection pulse. The liquid crystal molecules will be relaxed to either ϕ or $\phi+2\pi$ depending on the magnitude of the selection pulse.[11]

For transmissive BTN, the bistable twist states are ϕ and $\phi+2\pi$, and ϕ should be $-\pi$, $-\pi/2$, 0, $\pi/2$, π, ...[6,8] For the case of reflective BTN's without a rear polarizer, these angles are no longer the optimal angles. The optimal design parameters for a reflective BTN must be determined. The reflectance, R of a single polarizer reflective BTN was calculated in terms of Berreman's 4x4 matrix method.[12] The director profiles of the two bistable states were solved by minimizing the Frank-Oseen elastic energy.[13] The parameter space of reflective BTN displays was generated as a special case of the dynamic parameter space method,[14] when zero applied voltage was chosen. The two bistable states of the reflective BTN

devices were studied for the optical properties regardless of switching mechanism, since the two bistable states were stable or metastable at zero voltage. The reflectance parameter space was calculated by varying ϕ (the twisted angle) and $d\Delta n$ (the product of cell thickness, d and birefringence, Δn) with β, the polarizer angle fixed. ϕ ranged from $-\pi$ to π for one stable state and from π to 3π for the other stable state. The twist angles of the two stable states have a difference of 2π. The contrast ratio was defined to be always greater than or equal to one. It was either $R(\phi)/R(\phi+2\pi)$ or $R(\phi+2\pi)/R(\phi)$, depending on which reflectance was smaller, $R(\phi)$ or $R(\phi+2\pi)$.

The liquid crystal material parameters used in this calculation are the following: $K_{11}=12.4\times10^{-12}$N, $K_{22}=6.0\times10^{-12}$N, $K_{33}=17.1\times10^{-12}$N; $\varepsilon_{\perp}=6.6$, $\varepsilon_{11}=13.8$; pretilt angle is 2^0; cell thickness, d of 5 μm. The pitch is varied with the twisted angle and is equal to $2\pi d/\phi$. These are typical values for supertwisted namatic liquid crystal mixtures.

The quarter wave plate was modeled as an anisotropic layer whose $d\Delta n$ value was equal to $\lambda/4$. λ is equal to 550 nm. The angle of the fast axis of the quarter wave plate is α.

3. REFLECTIVE BTN WITH FRONT QUARTER WAVE PLATE

A simple geometry of the reflective BTN device was assumed for constructing the parameter space. The polarizer and input director were assumed along the same direction. The liquid crystal had a right-handed twist along the incidence direction of light. The cell added a quarter wave plate between the polarizer and the liquid crystal cell. The fast axis of the plate made 45° with respect to the input director (α=45°). An ideal polarizer with no absorption was modeled. The director profile was solved for each twisted angle, ϕ from $-180°$ to 180° for one stable state and ϕ from 180° to 540° for the other stable state. The optical properties were calculated for each twisted angle with $d\Delta n$ ranging from 0 to 1.5 μm in increments of 0.025 μm. The wavelength used in all the calculations was centered at 550 nm. The reflectance was averaged for 81 different wavelengths equally spaced in the region (546 nm, 554 nm).

Figure 1(a) shows a contour map of the contrast ratio $R(\phi)/R(\phi+2\pi)$ as a function of $d\Delta n$ and ϕ. In this case φ is between $-\pi$ and π. Figure 1(b) shows a contour map of the contrast ratio $R(\phi+2\pi)/R(\phi)$. These two graphs are reciprocals of each other. From definitions, valleys in figure 1(a) need to be emphasized so the reciprocals are plotted in figure 2(b). The viewing angle is 0°. In the parameter space representations, the viewing angle is usually 0° unless specified otherwise. There are several islands of high contrast in the $d\Delta n$ and ϕspace. Two typical modes A

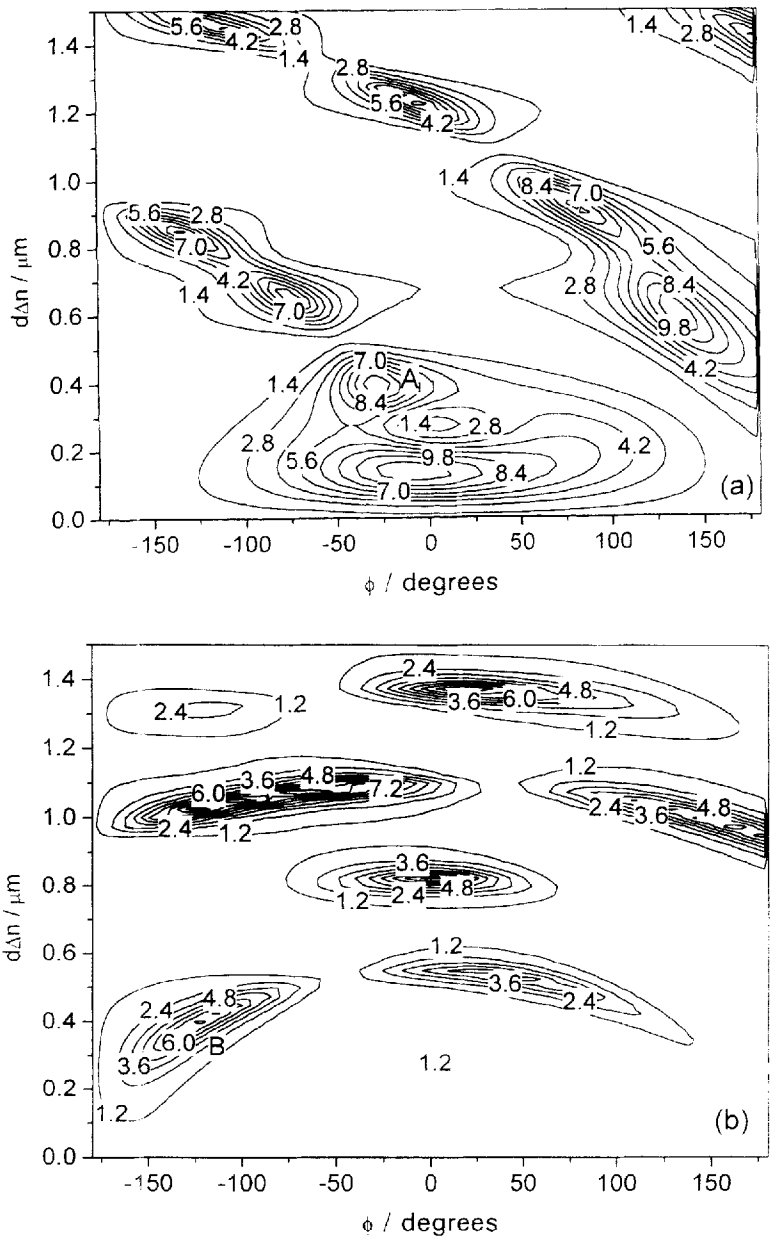

FIGURE 1 Contrast ratio contour plot for reflective BTN display with front quarter wave plate (a) $R(\phi)/R(\phi+2\pi)$; (b) $R(\phi+2\pi)/R(o)$

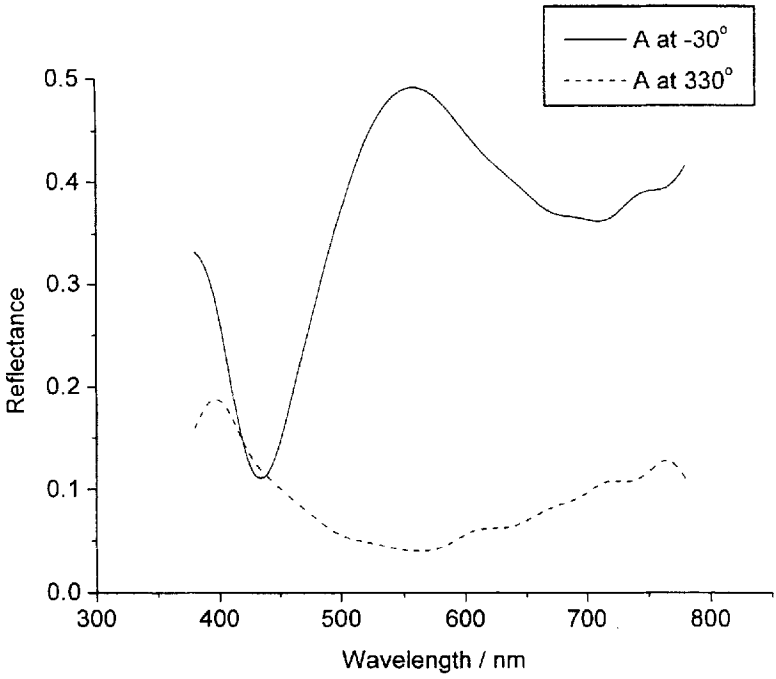

FIGURE 2 Reflectance spectra for mode A at two bistable states

in figure 1(a) and B in figure 1(b) will be discussed. These represent two of the more visible islands. A labels the island that occurs at (ϕ=-30°, dΔn= 0.4 μm), while B labels the island that occurs at (ϕ=-120°, d$\triangle$n= 0.4 μm). The calculated reflectance spectra of mode A in two bistable states R(-30°) and R(330°) is shown in figure 2. The reflectance spectra of mode B in two bistable states R(-120°) and R(240°) is shown in figure 3. These two mode have dΔn values of 0.4 μm. For comparison, The value of dΔn for the non-compensated reflective BTN is around 0.2 μm.[10] The increasing of dΔn value of the compensated reflective BTN means a larger cell thickness and easier cell fabrication. The mode A is a better choice regarding brightness and wavelength dispersion.

4. REFLECTIVE BTN WITH REAR QUARTER WAVE PLATE

The cell studied added a quarter wave plate between the liquid crystal cell and the reflector. The polarizer and input director were assumed to be along the same

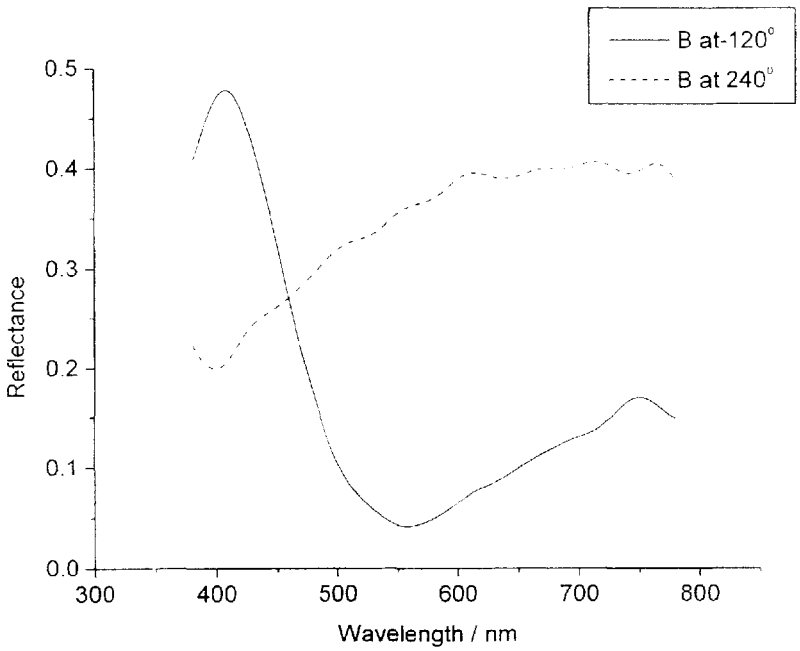

FIGURE 3 Reflectance spectra for mode B at two bistable states

direction and the liquid crystal had a right-handed twist along the incidence direction of the light.

First, the case of the fast axis of the quarter wave plate making 45° to the input director direction is studied. Figure 4(a) shows a contour map of the contrast ratio $R(\phi)/R(\phi+2\pi)$ as a function of $d\Delta n$ and for $\beta=0°$ and $\alpha=45°$. Figure 4(b) shows a contour map of the contrast ratio $R(\phi+2\pi)/R(\phi)$ as a function of $d\Delta n$ and ϕ for $\beta=0°$ and $\alpha=45°$. Two typical modes: C in figure 4(a) and D in figure 4(b) will be discussed. C represents the island that occurs at ($\phi=-86°$, $d\Delta n= 0.75\ \mu m$), while D represents the island that occurs at ($\phi=0°$, $d\Delta n= 0.675\ \mu m$). The calculated reflectance spectra of mode C in two bistable states R(-86°) and R(274°) is shown in figure 5. The reflectance spectra of mode D in two bistable states R(0°) and R(360°) is shown in figure 6.

Second, the case of the fast axis of quarter wave plate making 0° to the input director direction is discussed. Figure 7(a) shows a contour map of the contrast ratio $R(\phi)/R(\phi+2\pi)$ as a function of $d\Delta n$ and ϕ for $\beta=0°$ and $\alpha=0°$. Figure 7(b) shows a contour map of the contrast ratio $R(\phi+2\pi)/R(\phi)$ as a function of $d\Delta n$ and ϕ for $\beta=0°$ and $\alpha=0°$. Two typical modes: E in figure 7(a) and F in figure 7(b)

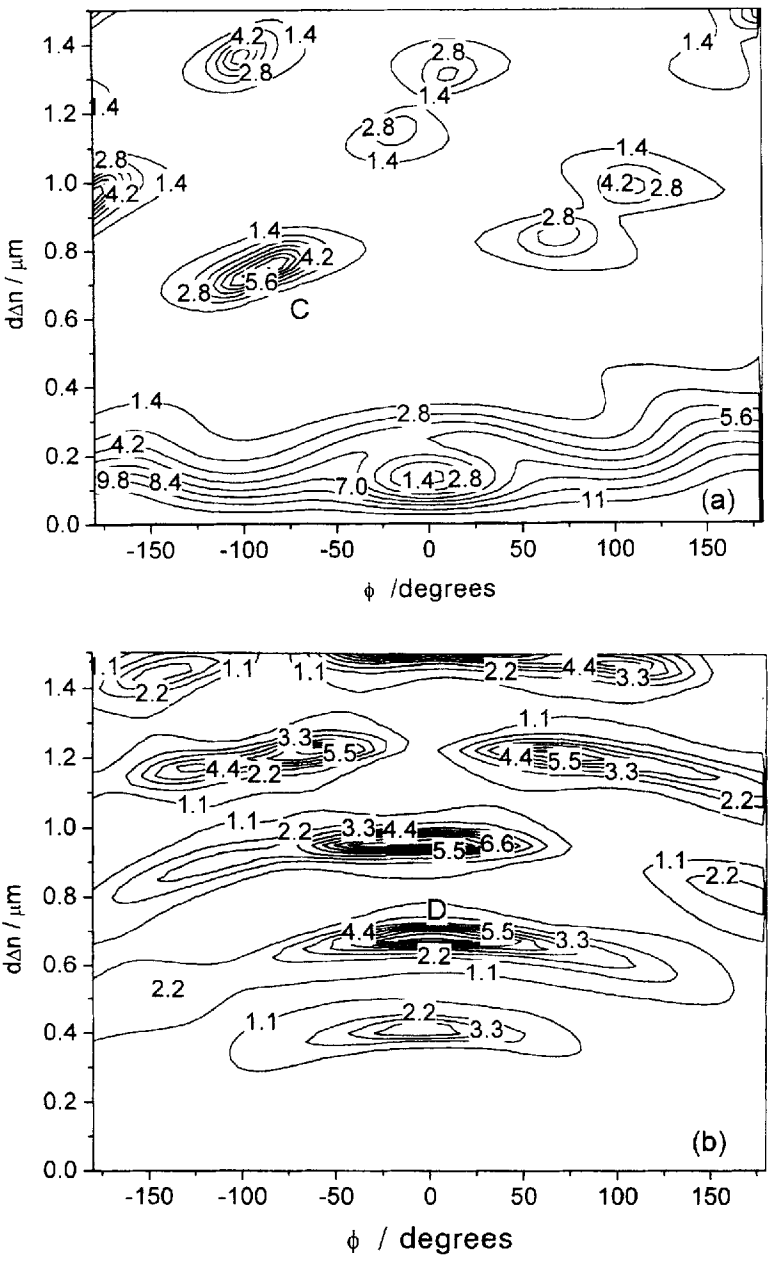

FIGURE 4 Contrast ratio contour plot for reflective BTN display with rear quarter wave plate (α=45°) (a) $R(\phi)/R(\phi+2\pi)$; (b) $R(\phi+2\pi)/R(\phi)$

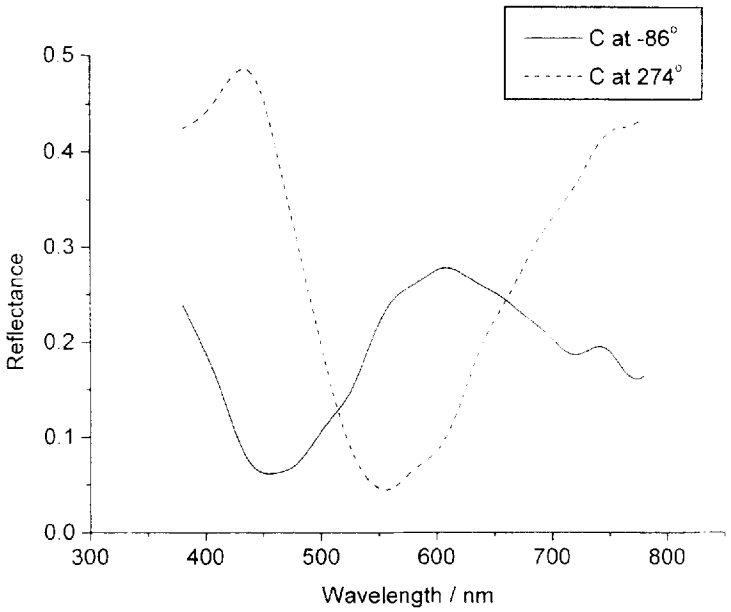

FIGURE 5 Reflectance spectra for mode C at two bistable states

will be discussed. E labels the island that occurs at (ϕ=120°, dΔn= 0.65 μm), while F labels the island that occurs at (ϕ=-128°, dΔn= 0.35 μm). The calculated reflectance spectra of mode E in two bistable states R(120°) and R(480°) is shown in figure 8. The reflectance spectra of mode F in two bistable states R(-128°) and R(232°) is shown in figure 9.

Mode D is the best operation mode of these four modes studied. It has a large dΔn value of 0.675 μm. The wavelength dispersion of reflectance is small as compared to other three modes. And the bright state has high light efficiency. The viewing angle dependence of contrast ratio was also calculated for the mode D as shown in figure 10. The contrast ratio is larger than 4.0 within viewing angle ±50°.

5. CONCLUSIONS

Film compensated reflective BTN displays were studied by using a parameter space method. Both front and rear film compensated reflective BTN displays were optimized in terms of contrast ratio and wavelength dispersion of reflectance.

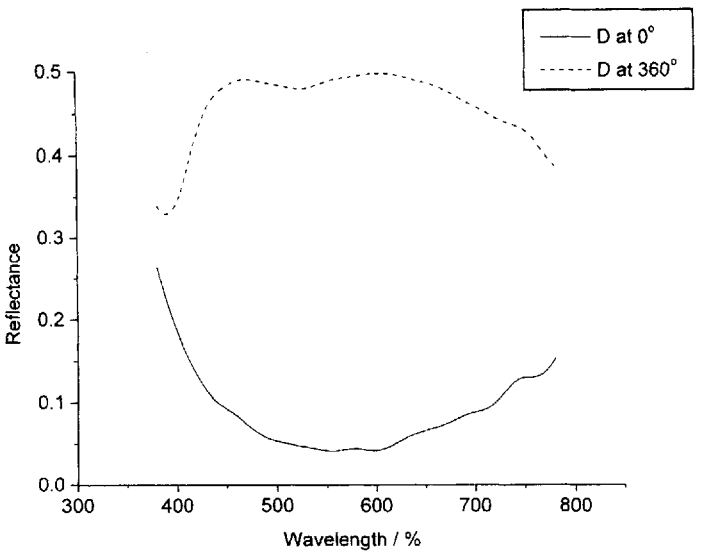

FIGURE 6 Reflectance spectra for mode D at two bistable states

The strong dispersion of non-compensated reflective BTN displays limits its operation conditions having small dΔn value around 0.2 μm. Film compensation of reflective BTN displays provides more choices of operation modes. These operation modes have large d△n value. The front film compensation has the advantage of placing the reflector inside the liquid crystal cell so that pallax could be rempved. The rear film compensation is also used in many liquid crystal devices. Our results provide a basis for the comparison between these two different compensation configurations and we believe these results will be helpful in realization of optimum reflective BTN devices.

For the reflective BTN with front quarter wave plate, mode A at (ϕ=-30°, dΔn= 0.4 μm) is an optimized operating condition; for the reflective BTN with rear quarter wave plate, mode D at (ϕ=0°, dΔn= 0.675 μm) is an optimized operation mode.

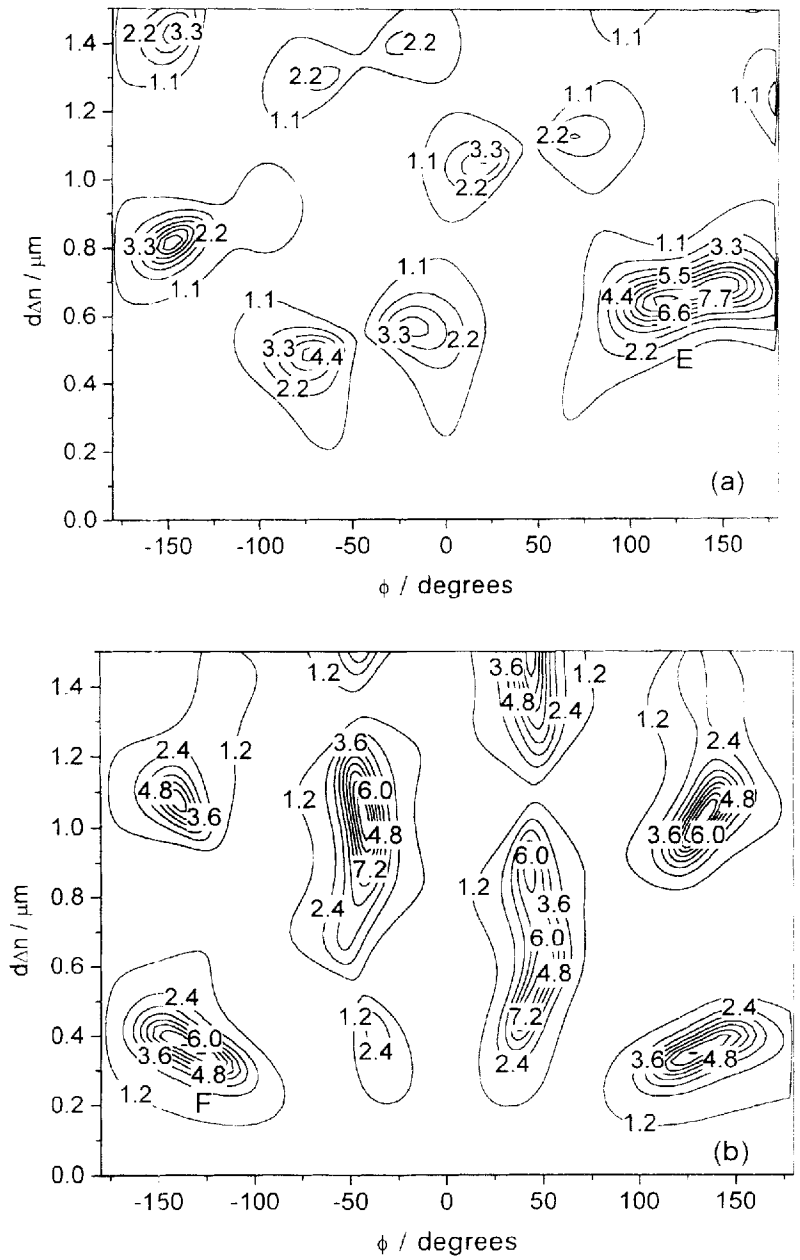

FIGURE 7 Contrast ratio contour plot for reflective BTN display with rear quarter wave plate (α=0°) (a) $R(\phi)/R(\phi+2\pi)$; (b) $R(\phi+2\pi)/R(\phi)$

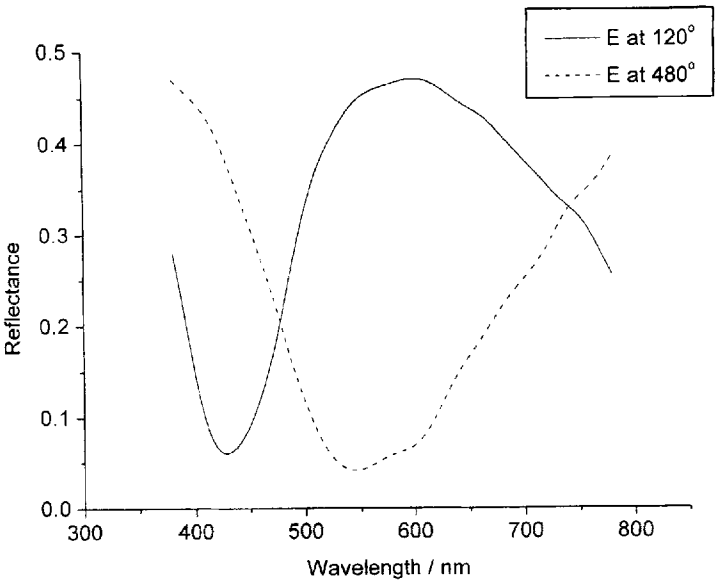

FIGURE 8 Reflectance spectra for mode E at two bistable states

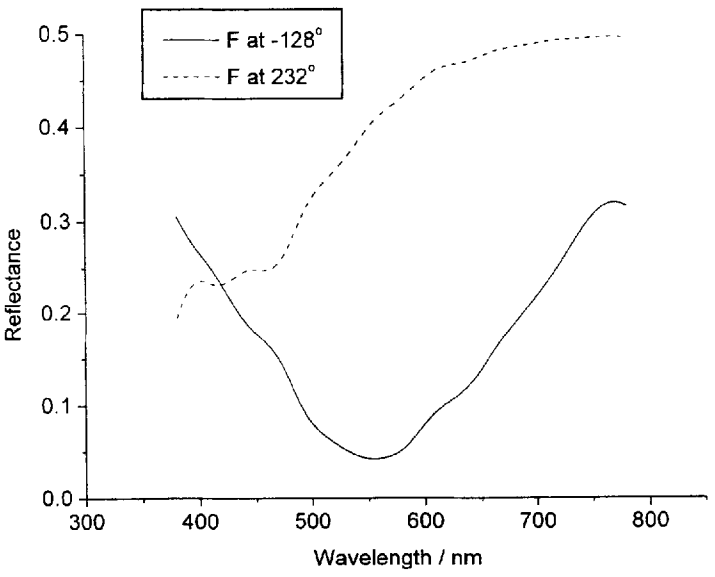

FIGURE 9 Reflectance spectra for mode F at two bistable states

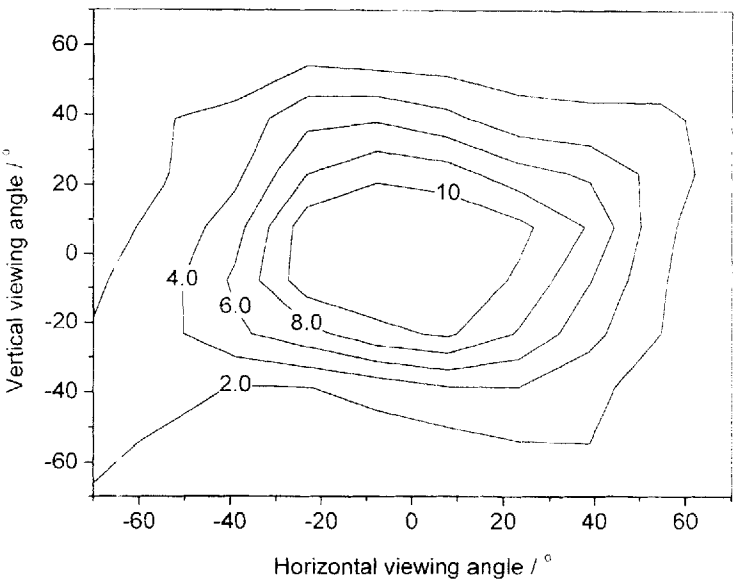

FIGURE 10 Viewing angle dependence of the contrast ratio for mode D

References

1. D.W. Berreman and W.R. Heffner, *Appl. Phys. Lett.* **37**, 109 (1980).
2. D.W. Berreman and W.R. Heffner, *J. Appl. Phys.* **52**, 3032 (1981).
3. T. Tanaka, Y. Sato, A. Inoue, Y. Momose, H. Nomura, and S. Iino, *Asia Display 95 Digest* p. 259 (1995).
4. T. Tanaka, Y. Sato, T. Obikawa, H. Nomura, and S. Iino, *IDRC 97 Digest* p. M-64 (1997).
5. J.C. Kim, G.-J. Choi, Y.-S. Kim, K.H. Kang, T.-H. Yoon, K.G. Nam, H.S. Kim, and E.-S. Lee, *SID 97 Digest*p. 33 (1997).
6. T.Z. Qian, Z.L. Xie, H.S. Kwok, and P. Sheng, *Appl. Phys. Lett.* **71**, 596 (1997).
7. C.D. Hoke, J. Li, J.R. Kelly, and P.J. Bos, *Jpn. J. Appl. Phys.* **36**, L227 (1997).
8. Z-L Xie and H.S. Kwok, *Jpn J. Appl. Phys.* **37**, 2572 (1998).
9. Y. J. Kim, Z. Zhuang, J.S. Patel, *SID 99 Digest* p. 866 (1999).
10. H.F. Cheng and H.J. Gao, *J. Appl. Phys.* **87**, 7476 (2000).
11. G.D. Lee, G-H. Kim, K-H. Park, K-C. Chang, T-H. Yoon, J.C. Kim, *SID 99 Digest* p. 862 (1999).
12. D.W. Berreman, *J. Opt. Soc. Am.* **62**, 502 (1972).
13. A. Sugimura, G.R. Luckhurst and O.-Y. Zhong-can, *Phys. Rev.* **E52**, 681 (1995).
14. H.F. Cheng, H.J. Gao and F.S. Zhou, *J. Appl. Phys.* **86**, 5953 (1999).